J|A|C|S
ARTICLES
Published on Web 09/23/2004

# Valence Bond Calculations of Hydrogen Transfer Reactions: A General Predictive Pattern Derived from Theory

Peifeng Su,[†] Lingchun Song,[†] Wei Wu,*[,†] Philippe C. Hiberty,[‡] and Sason Shaik*[,§]

*Contribution from the State Key Laboratory of Physical Chemistry of Solid Surfaces, Center for Theoretical Chemistry, and Department of Chemistry, Xiamen University, Xiamen 361005, P. R. China, Laboratoire de Chimie Physique, Groupe de Chimie Théorique, Université de Paris-Sud, 91405 Orsay Cédex, France, and Department of Organic Chemistry and the Lise Meitner-Minerva Center for Computational Quantum Chemistry, The Hebrew University, Jerusalem 91904, Israel*

Received April 2, 2004; E-mail: weiwu@xmu.edu.cn

***Abstract:*** Hydrogen abstraction reactions of the type $X^{\bullet} + H-H' \rightarrow X-H + H'^{\bullet}$ (X = F, Cl, Br, I) are studied by ab initio valence bond methods and the VB state correlation diagram (VBSCD) model. The reaction barriers and VB parameters of the VBSCD are computed by using the breathing orbital valence bond and valence bond configuration interaction methods. The combination of the VBSCD model and semiempirical VB theory *leads to analytical expressions for the barriers and other VB quantities that match the ab initio VB calculations fairly well*. The barriers are influenced by the endo- or exothermicity of the reaction, but the fundamental factor of the barrier is the average singlet−triplet gap of the bonds that are broken or formed in the reactions. Some further approximations lead to a simple formula that *expresses the barrier for nonidentity and identity hydrogen abstraction reactions as a function of the bond strengths of reactants and products*. The semiempirical expressions are shown to be useful not only for the model reactions that are studied in this work, but also for other nonidentity and identity hydrogen abstraction reactions that have been studied in previous articles.

## Introduction

One of the most fundamental reactions is hydrogen abstraction that plays a significant role in a variety of important chemical and biological processes.[1−11] This added allure and the relative simplicity of the process have attracted a significant theoretical activity in this field.[12−44] Understanding reactivity patterns of hydrogen abstraction reactions has become therefore a goal of considerable practical and conceptual values. Theorists and practicing chemists have gained significant insight into the key

[†] Xiamen University.
[‡] Université de Paris-Sud.
[§] The Hebrew University.

(1) Groves, J. T. *Proc. Natl. Acad. Sci. U.S.A.* **2003**, *100*, 3569−3574.
(2) *Biomimetic Oxidations Catalyzed by Transition Metal Complexes*; Meunier, B. M., Ed.; Imperial College Press: London, 2000.
(3) Klinman, J. P. *Pure Appl. Chem.* **2003**, *75*, 601−608.
(4) Borman, S. *Chem. Eng. News.* **1994**, *72* (April 18), 4−5.
(5) Giese, B.; Graph, X. B.; Burger, J.; Kesselheim, J.; Senn, M.; Schäfer, T. *Angew. Chem., Int. Ed.* **1993**, *32*, 1742−1743.
(6) Groves, J. T. *J. Chem. Educ.* **1985**, *62*, 928−931.
(7) Halliwell, B.; Gutteridge, J. M. C. *Free Radicals in Biology and Medicine*, 2nd ed.; Clarendon Press: Oxford, 1989.
(8) Varadarajan, S.; Kanski, J.; Aksenova, M.; Lauderback, C.; Butterfield, D. A. *J. Am. Chem. Soc.* **2001**, *123*, 5625−5631.
(9) Rauk, A.; Armstrong, D. A.; Fairlie, D. P. *J. Am. Chem. Soc.* **2000**, *122*, 9761−9767.
(10) Hoffner, J.; Schottelius, M. J.; Feichtinger, D.; Chen, P. *J. Am. Chem. Soc.* **1998**, *120*, 376−385.
(11) Fokin, A. A.; Schreiner, P. R. *Chem. Rev.* **2002**, *102*, 1551−1594.
(12) Parr, C. A.; Truhlar, D. G. *J. Phys. Chem.* **1971**, *75*, 1844−1860.
(13) Benneyworth, P. R.; Balint-Kurti, G. G.; Davis, M. J.; Williams, I. H. *J. Phys. Chem.* **1992**, 96, 4346−4353.
(14) Tang, B.; Yang, B.; Han, K.; Zhang, R.; Zhang. J. *J. Chem. Phys.* **2000**, *113*, 10105−101113.
(15) (a) Dunning, T. H. *J. Phys. Chem.* **1984**, *88*, 2469−2477. (b) Dunning, T. H. *J. Chem. Phys.* **1977**, *66*, 2752−2753.
(16) Last, I.; Baer, M. *J. Chem. Phys.* **1984**, *80*, 3246−3252.
(17) Alexander, M. H.; Capecchi, G.; Werner, H. J. *Science* **2002**, *296*, 715−718.
(18) (a) Bender, C. F.; Garrison, B. J.; Schaefer, H. F., III. *J. Chem. Phys.* **1975**, *62*, 1188−1189. (b) Frish, M. J.; Liu, B.; Binkley, J. S.; Schaefer, H. F., III.; Miller, W. H. *Chem. Phys. Lett.* **1985**, *114*, 1−5.
(19) Botschwina, P.; Meyer, W. *J. Chem. Phys.* **1977**, *67*, 2390−2391.
(20) Basch, H.; Hoz, S. *J. Phys. Chem. A* **1997**, *101*, 4416−4431.
(21) Skokov, S.; Wheeler, R. A. *Chem. Phys. Lett.* **1997**, *271*, 251−258.
(22) (a) Tarchouna, Y.; Bahri, M.; Jaidane, N.; Lakhdar, Z. B.; Flament, J. P. *J. Mol. Struct. (THEOCHEM)* **2003**, *664*, 189−196. (b) Bahri, M.; Tarchouna, Y.; Jaidane, N.; Lakhdar, Z. B.; Flament, J. P. *J. Mol. Struct. (THEOCHEM)* **2003**, *664*, 229−236.
(23) Porezag, D.; Pederson, M. R. *J. Chem. Phys.* **1995**, *102*, 9345−9349.
(24) Fox, G. L.; Schlegel, H. B. *J. Phys. Chem.* **1992**, *96*, 298−302.
(25) (a) Jursic, B. S. *Chem. Phys. Lett*. **1995**, *244*, 263−268. (b) Jursic, B. S. *Chem. Phys. Lett.* **1996**, *256*, 603−608.
(26) Chen, Y.; Tschuikov-Roux, E. *J. Phys. Chem.* **1993**, *97*, 3742−3749.
(27) Litivinowicz, J. A.; Ewing, D. E.; Jurisevic, S.; Manka, M. J. *J. Phys. Chem.* **1995**, *99*, 9709−9716.
(28) Gonzales, C.; McDougall, J. J. W.; Schlegel, H. B. *J. Phys. Chem*. **1990**, *94*, 7467−7471.
(29) Dobbs, K. D.; Dixon, D. A.; Komornicki, A. *J. Chem. Phys.* **1993**, *98*, 8852−8858.
(30) (a) Melissas, V. S.; Truhlar, D. G. *J. Phys. Chem.* **1994**, *98*, 875−886. (b) Melissas, V. S.; Truhlar, D. G. *J. Chem. Phys.* **1993**, *99*, 1013−1027.
(31) Corchado, J. C.; Olivares del Valle, F. J.; Espinosa-Garcia, J. *J. Phys. Chem.* **1993**, *97*, 9129−9132.
(32) Davis, L. P.; Burggraf, L. W.; Gordon, M. S.; Baldridge, K. K. *J. Am. Chem. Soc.* **1985**, *107*, 4415−4419.
(33) Corchado, J. C.; Espinosa-Garcia, J. *J. Chem. Phys.* **1996**, *105*, 3152−3159.
(34) Louis, F.; Rayez, M. T.; Rayez, J. C.; Sawerysyn, J. P. *Phys. Chem. Chem. Phys.* **1999**, *1*, 383−389.
(35) Bottoni, A.; Poggi, G. *J. Mol. Struct. (THEOCHEM)* **1995**, *337*, 161−172.
(36) Truong, T. N.; Truhlar, D. G.; Baldridge, K. K.; Gordon, M. Steckler, R. *J. Chem. Phys.* **1989**, *90*, 7137−7142.
(37) Dobbs, K. D.; Dixon, D. A. *J. Phys. Chem.* **1994**, *98*, 12584−12589.

features of the process by using different models based on a variety of factors such as bond energies, Pauli repulsion, "polar effects" (or ionic effects), steric effects, and so on.[45−65] Nevertheless, the questions of the origin of barriers and the characteristics of the transition state (TS) have remained the central theoretical issues. In this sense, a suitable *quantum chemical model* should provide a clear mechanism of barrier and transition-state formation and at the same time lead to a compact expression of the barrier with explicit dependence on fundamental properties of the reactants. Such models have traditionally emerged from valence bond (VB) theory and its various semiempirical implementations.[66−74]

As part of a long-term program to model chemical reactivity on the basis of modern VB methods, we have undertaken an approach that uses the VB state correlation diagram (VBSCD)[67] as the means to model and reproduce barriers computed by ab initio VB methods, with an aim to establish gradually a general structure−reactivity expression. As a first step, we applied the breathing orbitals VB (BOVB) method[75] to the calculations and modeling of barriers of identity reactions, where the hydrogen is transferred between two identical groups (namely, identity reactions):[70]

$$X^{\bullet} + H-X \rightarrow X-H + X^{\bullet} \quad (X = CH_3,\ SiH_3,\ GeH_3,\ SnH_3,\ \text{and}\ PbH_3) \quad (1)$$

A simple expression for the barrier was derived on the basis of the VBSCD. In accord with previous conclusions,[13,53−57] it was shown that the organizing quantity of the identity barriers is the singlet−triplet excitation energy of the X−H bond that undergoes activation. Since the bond energy and the singlet−triplet excitation are related by simple proportionality, *the identity barrier was found to correlate also with the bond strength of the bond that is exchanged in the process*. The "polar effects", due to the mixing of ionic structures in the TS, were found to be significant, but were virtually constant in the series.[70,71]

In a subsequent treatment,[73] we applied the BOVB method to the computations of barriers for the nonidentity hydrogen transfer reactions between two different groups X and X′, in eq 2.

$$X'^{\bullet} + H-X \rightarrow X'-H + X^{\bullet} \quad (X' \neq X = CH_3,\ SiH_3,\ GeH_3,\ SnH_3,\ \text{and}\ PbH_3) \quad (2)$$

It was shown that the avoided crossing state (ACS), defined as that point on the reaction profile in which the energies of the reactant's and product's Lewis structures are identical, formed a reasonable approximation to the BOVB transition state. Using the ACS enabled the derivation of semiempirical expressions for resonance energy, for height of crossing point, and for the reaction barrier. These estimated VB quantities were shown to match quite well the values calculated by ab initio VB theory. Much as for the corresponding identity reactions, here too the "polar effect" behaved as a quasi-constant quantity.

One of the appealing features of the VBSCD equation for the nonidentity barrier was its transformation to an expression akin to the Marcus equation,[76,77] as a balance between an intrinsic quantity and the reaction driving force (given by the bond strength difference between the exchanging bonds, H−X and H−X′). Using the VBSCD, the intrinsic quantity of the barrier can be independently determined, again from singlet−triplet excitation energies of the H−X and H−X′ bonds. Since the bond energies are proportional to the singlet−triplet excitations, one expects also good correlations of barriers with bond


(38) Duncan, W. T.; Truong, T. N. *J. Chem. Phys.* **1995**, *103*, 9642−9652.
(39) Chen, Y. H.; Tschuikow-Roux, E.; Rauk, A. *J. Phys. Chem.* **1991**, *95*, 9832−9836.
(40) Guha, S.; Francisco, J. S. *J. Mol. Struct. (THEOCHEM)* **2001**, *573*, 171−180.
(41) Ogliaro, F.; Harris, N.; Cohen, S.; Filatov, M.; de Visser, S. P.; Shaik, S. *J. Am. Chem. Soc.* **2000**, *122*, 8977−8989.
(42) Kamachi, T.; Yoshizawa, K. *J. Am. Chem. Soc.* **2003**, *125*, 4652−4661.
(43) Torrent, M.; Musaev, D. G.; Basch, H.; Morokuma, K. *J. Comput. Chem.* **2002**, *23*, 59−76.
(44) Siegbahn, P. E. M.; Crabtree, R. H. *J. Am. Chem. Soc.* **1997**, *119*, 3103−3113.
(45) (a) Clarke, J. S.; Rypkema, H. A.; Kroll, J. H.; Donahue, M. N.; Anderson, J. G. *J. Phys. Chem. A* **2000**, *104*, 4458−4468. (b) Donahue, M. N.; Clarke, J. S.; Anderson, J. G. *J. Phys. Chem. A* **1998**, *102*, 3923−3933. (c) Donahue, M. N. *Chem. Rev.* **2003**, *103*, 4593−4604.
(46) Johnston, H. S.; Parr, C. *J. Am. Chem. Soc.* **1963**, *85*, 2544−2551.
(47) (a) Zavitsas, A. A. *J. Am. Chem. Soc.* **1972**, *94*, 2779−2789. (b) Zavitsas, A. A.; Chatgilialoglu, C. *J. Am. Chem. Soc.* **1995**, *117*, 10645−10654. (c) Zavitsas, A. A. *J. Am. Chem. Soc.* **1998**, *120*, 6578−6586.
(48) Blowers, P.; Masel, R. I. *J. Phys. Chem. A* **1998**, *102*, 9957−9964.
(49) Lee, W. T.; Masel, R. I. *J. Phys. Chem.* **1996**, *100*, 10945−10951.
(50) (a) Mayer, J. M. In *Biomimetic Oxidations Catalyzed by Transition Metal Complexes*; Meunier, B. M., Ed.; Imperial College Press: London, 1999; Chapter 1, pp 1−44. (b) Gardner, K. A.; Mayer, J. M. *Science* **1995**, *269*, 1849−1851. (c) Bryant, J. R.; Mayer, J. M. *J. Am. Chem. Soc.* **2003**, *125*, 10351−10361. (d) Roth, J. P.; Yoder, J. C.; Won, T.; Mayer, J. M. *Science* **2001**, *294*, 2524−2526. (e) Mayer, J. M. *Acc. Chem. Res.* **1998**, *31*, 441−450.
(51) Kim, Y.; Corchado, J. C.; Villa, J.; Xing, J.; Truhlar, D. G. *J. Chem. Phys.* **2000**, *112*, 2718−2735.
(52) Roberts, B. P. *J. Chem. Soc., Perkin Trans. 2* **1996**, 2719−2725.
(53) Pross, A.; Yamataka, H.; Nagase, S. *J. Phys. Org. Chem.* **1991**, *4*, 135−140.
(54) Maitre, P.; Hiberty, P. C.; Ohanessian, G.; Shaik, S. *J. Phys. Chem.* **1990**, *94*, 4089−4093.
(55) Shaik, S.; Hiberty, P. C. In *Theoretical Models for Chemical Bonding*; Maksic, Z. B., Ed.; Springer-Verlag: Heidelberg: Germany, 1991; Vol. 4, p 269.
(56) Shaik, S.; Hiberty, P. C. *Adv. Quantum Chem.* **1995**, *26*, 99−163.
(57) Pross, A. *Theoretical and Physical Principles of Organic Reactivity*; Wiley & Sons: New York, 1995; pp 83−124; 235−290.
(58) Pross, A. *Adv. Phys. Org. Chem.* **1985**, *21*, 99−196.
(59) Salikhov, A.; Fischer, H. *Theor. Chim. Acta* **1997**, *96*, 114−121.
(60) Fischer, H.; Radom, L. *Angew. Chem.* **2001**, *40*, 1340−1371.
(61) Harcourt, R. D.; Ng, R. *J. Phys. Chem.* **1993**, *97*, 12210−12214.
(62) Harcourt, R. D. *J. Phys. Chem. A* **2003**, *107*, 10324−10329.
(63) Sharter, A. B.; Tian, F.; Dolbier, W. R., Jr.; Smart, B. E. *J. Am. Chem. Soc.* **1999**, *121*, 7335−7341.
(64) Hrovat, D. A.; Borden, W. T. *J. Am. Chem. Soc.* **1994**, *116*, 6459−6460.
(65) (a) Russell, G. A. *J. Org. Chem.* **1958**, *23*, 1407−1409. (b) Russell, G. A. In *Free Radicals*; Kochi, J. K., Ed.; Wiley & Sons: New York, 1973; Vol 1, pp 293−298. (c) Walling, C. In *Free Radicals*; Wiley & Sons: New York, 1973; Chapter 8.
(66) London, F. *Z. Elekrochem.* **1929**, *35*, 552.
(67) Shaik, S.; Shurki, A. *Angew. Chem., Int. Ed.* **1999**, *38*, 586−625.
(68) Shaik, S. *J. Am. Chem. Soc.* **1981**, *103*, 3692−3701.
(69) Warshel, A.; Weiss, R. M. *J. Am. Chem. Soc.* **1980**, *102*, 6218−6226.
(70) Shaik, S.; Wu, W.; Dong, K.; Song, L.; Hiberty, P. C. *J. Phys. Chem. A* **2001**, *105*, 8226−8235.
(71) Shaik, S.; de Visser, S. P.; Wu, W.; Song, L.; Hiberty, P. C. *J. Phys. Chem. A* **2001**, *106*, 5043−5045.
(72) Wu, W.; Shaik, S.; Saunder, W. H. *J. Phys. Chem. A* **2002**, *106*, 11616−11370.
(73) Song, L.; Wu, W.; Dong, K.; Hiberty, P. C.; Shaik, S. *J. Phys. Chem. A* **2002**, *106*, 11361−11370.
(74) Wu, W.; Danovich, D.; Shurki, A.; Shaik, S. *J. Phys. Chem. A* **2000**, *104*, 8744−8758.
(75) (a) Hiberty, P. C.; Flament, J. P. J.; Noizet, E. *Chem. Phys. Lett.* **1992**, *189*, 259−265. (b) Hiberty, P. C.; Humbel, S.; Byrman, C. P.; Van Lenthe, J. H. *J. Chem. Phys.* **1994**, *101*, 5969−5976. (c) Hiberty, P. C.; Humbel, S.; Archirel, P. *J. Phys. Chem.* **1994**, *98*, 11697−11704. (d) Hiberty, P. C.; Shaik, S. *Theor. Chim. Acc.* **2002**, *108*, 255−272. (e) Hiberty, P. C. In *Molden Electronic Structure Theory and Applications in Organic Chemistry*; Davidson, E. R., Ed.; Word Scientific River Edge: New York, 1997; pp 289−267. (f) Hiberty, P. C.; Shaik, S. In *Valence Bond Theory*; Cooper, D. L., Ed.; Elsevier: Amsterdam, 2002; pp 187−225.
(76) (a) Marcus, R. A. *Faraday. Discuss. Chem. Soc.* **1960**, *29*, 21−31. (b) Formosinho, S. J.; Arnaut, L. R.; Fausto, R. *Prog. React. Kinet.* **1998**, *23*, 1−90. (c) Eberson, L. *Electron-Transfer Reactions in Organic Chemistry*; Springer-Verlag: Berlin, 1987.
(77) Blowers, P.; Masel, R. I.; *J. Phys. Chem. A.* **1999**, *103*, 7047−7054.

energies in related reaction series as found amply by the extended Mayer correlations.[50]

Although the VBSCD equation, derived in refs 67 and 70, produces barriers in good agreement with the ab initio VB results for the sets of reactions in eqs 1 and 2, there remains the question of its general applicability. As a test of generality, we decide to apply the BOVB method[75] and a more recently developed multistructure VB method, VBCI,[78] to another series of hydrogen abstraction reactions, shown in eq 3, and to test the VBSCD equations on these reactions as well as on the entire set in eqs 1−3.

$$X^{\bullet} + H{-}H' \rightarrow X{-}H + H'^{\bullet} \quad (X = F, Cl, Br, I) \qquad (3)$$

The reactions in eq 3 have been widely studied in the field of reaction dynamics and quantum chemistry,[12−19] but to our knowledge, the reactions have never been studied by means of modern ab initio VB theory that is based on Heitler−London−Slater−Pauling functions *with all the ionic contributions included*. These reactions vary from highly endothermic in the case of iodide (X = I) to highly exothermic for the case of fluoride (X = F) and, as such, constitute a real challenge for the VB computational methods as well as for the VBSCD model. In brief, the aim of the present study is to apply the VBSCD model to understand the origin of barriers in the hydrogen transfer reactions specified by eq 3 and to derive general analytical expressions that will enable one to predict the barriers of these reaction and others in terms of easily accessible properties of the reactants and products.

## Theoretical Methods

**The Spin-Free Form of Valence Bond Theory.** The VB calculations use the spin-free formulation of quantum chemistry. The spin-free approach for VB theory has been fully described elsewhere[79,80] and will be sketched only briefly.

In spin-free VB theory, a many-electron wave function is expressed in terms of spin-free VB functions $\Phi_K$,

$$\Psi = \sum_K C_K \Phi_K \qquad (4)$$

$\Phi_K$ may be a bonded tableau (BT) state,[79] defined as

$$\Phi_K = N_K \, e_{r1}^{[\lambda]} \Omega_K \qquad (5)$$

where $N_K$ is a normalization factor, $e_{rs}^{[\lambda]}$ is a standard projector of the symmetric group $S_N$, defined through the irreducible representation matrix elements, $D_{rs}^{[\lambda]}(P)$, as

$$e_{rs}^{[\lambda]} = \left(\frac{f_\lambda}{N!}\right)^{1/2} \sum_P D_{rs}^{[\lambda]}(P) P \qquad (6)$$

where $f_\lambda$ is the dimension of the irreducible representation $[\lambda]$, and $\Omega_K$ is an orbital product,

$$\Omega_K = \phi_{k_1}(1)\phi_{k_2}(2)\phi_{k_3}(3)\cdots\phi_{k_N}(N) \qquad (7)$$

that maintains a one to one correspondence with the usual VB structures, by the arrangement of orbital indices.

With this permutation symmetry-adapted basis (eq 5), the Hamiltonian and overlap matrix elements are written, respectively, as eqs 8 and 9

$$H_{KL} = \langle \Phi_K | H | \Phi_L \rangle = \sum_{P \in S_N} D_{11}^{[\lambda]}(P) \langle \Omega_K | HP | \Omega_L \rangle \qquad (8)$$

$$M_{KL} = \langle \Phi_K | \Phi_L \rangle = \sum_{P \in S_N} D_{11}^{[\lambda]}(P) \langle \Omega_K | P | \Omega_L \rangle \qquad (9)$$

The coefficients $C_K$ in eq 4 are subsequently determined by solving the usual secular equation HC = *E*MC. Since VB structures are not mutually orthogonal, normalized structure weights are defined as:[81]

$$W_K = \sum_L C_K M_{KL} C_L \qquad (10)$$

In the VBSCF method,[82] both the VB orbitals $\phi_{ki}$ and structural coefficients $C_K$ are optimized simultaneously to minimize the total energy. The VBSCF method takes care of the static electron correlation but lacks dynamic correlation,[75d] an absolutely essential ingredient for the goal of quantitative accuracy. As such, VBSCF results are only qualitatively correct.

A VB method that incorporates dynamic correlation is the BOVB method.[75] BOVB improves the description of the VB structures by allowing different orbitals for different structures. In this manner, the orbitals can fluctuate in size and shape so as to fit the instantaneous charges of the atoms on which these orbitals are located. The method may be used at four possible levels, L-BOVB, SL-BOVB, D-BOVB, and SD-BOVB, of increasing accuracy and sophistication. For the sake of simplicity, the present article uses the level of D-BOVB, which is sufficiently accurate for reaction barriers but less accurate than VBCI for bond dissociation energies. For this reason, some of the discussion later is restricted to the VBCI results (e.g., Tables 4, 7, and 8).

The VBCI method[78] uses a configuration interaction technique to improve the energetic of a VBSCF calculation. A subsequent VBCI calculation involves the entire set of fundamental and excited VB structures. Similar to molecular orbital-based CI methods, the excited VB structures are generated by replacing occupied orbitals with virtual orbitals. The virtual orbitals are defined, by use of a projector, so as to be *strictly localized on precisely the same atom as the corresponding occupied orbitals.* In this manner, the entire VBCI wave function can be written as a linear combination of the same minimal number of VB structures as in the VBSCF and BOVB methods. In the present article, all calculations are carried out at the level of VBCISD that truncates the CI expansion beyond double excitation. This level has been shown to be definitely more accurate than the VBCIS level that involves only monoexcitations.[78]

**The VB Structure Set.** The hydrogen transfer reactions in eq 3 involve exchange of the H−H bond by H−X and reorganization of three electrons, which are required to attend the bond exchange. Scheme 1 shows all the modes of distributing three electrons among the three atoms. Structures **1**, **3**, and **5** correspond to the bonding mode of the reactants, while structures **2**, **4**, and **6** describe the products. Structures **7** and **8** are excited states that can mix into the TS but do not contribute to the reactants and products.

**The Reaction Coordinate.** The reaction coordinate *Q* is defined as the bond order difference:[70,73]

$$Q = n_1(d') - n_2(d), \; n(d) = e^{-a(d-d_0)} \qquad (11)$$

where constant *a* in $n(d)$ is taken from the corresponding value

(78) (a) Wu, W.; Song, L.; Cao, Z.; Zhang, Q.; Shaik, S. *J. Phys. Chem. A* **2002**, *106*, 2721−2726. (b) Song, L.; Wu, W.; Hiberty, P. C.; Danovich, D.; Shaik, S. *Chem.−Eur. J.* **2003**, *9*, 4540−4547. (c) Song, L.; Wu, W.; Zhang, Q.; Shaik, S. *J. Comput. Chem.* **2004**, *25*, 472−478.

(79) Wu, W.; Mo, Y.; Cao, Z.; Zhang, Q. A Spin-Free Approach for Valence Bond Theory and Its Application. In *Valence Bond Theory*; Cooper, D. L., Ed.; Elsevier: Amsterdam, 2002; pp 143−185.

(80) Li, X.; Zhang, Q. *Int. J. Quantum Chem.* **1989**, *36*, 599−632.

(81) Chirgwin, H. B.; Coulson, C. A. *Proc. R. Soc. London, Ser. A* **1950**, *2*, 196−209.

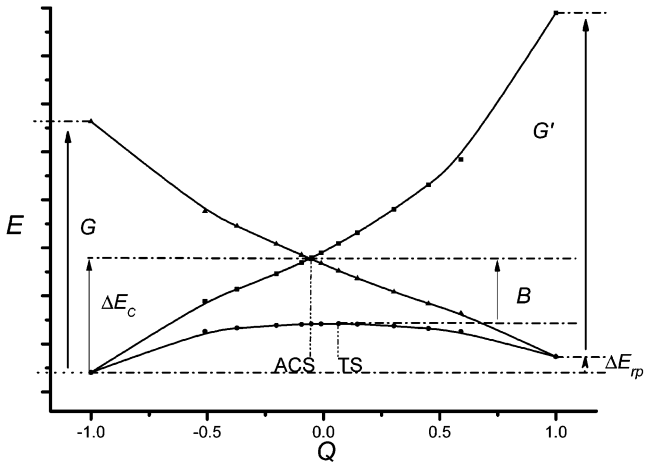


***Figure 1.*** A typical VBSCD for $X^{\bullet} + H-H' \rightarrow X-H + H'^{\bullet}$, exemplified by using the VB calculations for X = Cl.

***Scheme 1.*** VB Structure Set for Hydrogen Transfer Processes

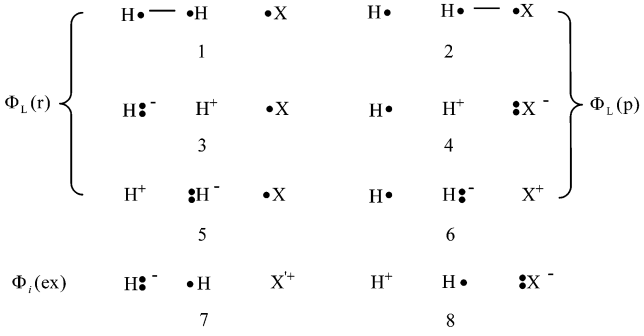


determined before for the identity reaction 1, for which the bond order was defined as 0.5 at the TS.[70,73] With this definition of $Q$, the path stretches from $-1$ to $+1$, as shown in Figure 1. Intrinsic reaction coordinate (IRC) calculations provide the relationship between the bond distances $d'$ (of H−H) and $d$ (of H−X). For a given value of $Q$, the individual $d'$ and $d$ lengths can be determined by combining the $d-d'$ relationship derived from the IRC with their relationship in eq 11.

**The VB State Correlation Diagram (VBSCD) Method.** The VBSCD[67] method uses VB theory to provide chemical insight into the barrier and other features of a chemical reaction. The central idea of the VBSCD approach is that the barriers of chemical reactions arise from an avoided crossing of VB configurations. The VBSCD in Figure 1 is composed of three curves: one is the adiabatic energy profile of the ground state that involves all eight structures in Scheme 1, and the other two are Lewis structures for the reactant and product, also called diabatic curves, respectively. The diabatic curves are determined variationally within the subset of VB structures in Scheme 1: covalent structure **1**, the two ionic structures **3** and **5** for reactants, covalent structure **2**, and the ionic structures **4** and **6** for products.[70] Thus, on the reactant's side of the diagram ($Q = -1$), the diabatic curve that represents the energy of the reactants' VB structure is merged with the ground state. This diabatic curve rises continuously as $Q$ increases and becomes an excited state on the product side of the diagram ($Q = 1$). This excited state is the image of the reactants in the products' geometry. Similarly, the other diabatic curve, featuring the energy change of the products' VB structure along the reaction coordinate, is drawn from the right-hand to the left-hand side of the diagram and reaches an excited state of the reactants. The quantity $G$ is the promotion energy from the ground state of the reactant to the excited state above it; an analogous quantity is the promotion energy at the products side. The two intersecting curves mix and avoid the crossing. If the ACS (Figure 1) is a good enough approximation to the TS, then we may analyze the barrier in terms of diabatic quantities, such as the promotion gap, $G$, the height of the crossing point, $\Delta E_c$, and the resonance energy of the TS, $B$.[67,70]

**The Semiempirical VB Method.** The semiempirical VB method[73,74] can provide qualitative guides required to understand trends about the chemical reactions. The energy of the bond is given by $-\lambda$, while the nonbonded repulsion is given by $\lambda_T$, where the subscript, T, refers to the triplet Pauli repulsion. We use these parameters to independently quantify the features of the ACS, such as resonance energy, $B$, and the height of crossing point, $\Delta E_c$.

**Basis Sets, Geometries, and Computational Levels.** The D95V* basis set, of double-$\zeta$ plus polarization quality, was used for X = F, while for the heavier analogues we used the Los Alamos effective core potential and matching basis set, LANL2DZ to which we added $d$-polarization functions. All the electrons in the inner shell were frozen at the level of Hartree−Fock method. The TSs were optimized at the MP2 level, and the IRC path was used then as the "reaction coordinate" for all the VB calculations. Subsequently, using eq 11 we located the ACS and carried out VB computations on the transition states and ACSs, as well as on the reactant's state, to determine barriers. We also performed CCSD(T) calculations on barriers of the reactions to compare with VB results. All the VB calculations, including VBSCF, BOVB, and VBCI levels, were done with the Xiamen Valence Bond (XMVB) package of programs.[83] The MP2 and CCSD(T) calculations were carried out using GAUSSIAN 98.[84]

## Results and Discussion

**Avoided-Crossing State and Transition States.** Ever since the formulation of transition-state theory, a lot of effort has been devoted to developing models for characterizing the TS because it controls the height of the reaction barriers. One of us (S.S.) developed an approach for defining the transition state of a chemical reaction by introducing the concept of an ACS.[85] The ACS is that point on the reaction surface that lies directly underneath the crossing point and is the state that arises by the mixing of the two Lewis structures at their crossing point. As such, the wave function of the ACS after avoided crossing is well defined, starting from the Lewis state in eq 12.

$$\Psi_L = N[\Phi_L(r) - \Phi_L(p)] \qquad (12)$$

Here $N$ is a normalization factor, and $\Phi_L(r)$ and $\Phi_L(p)$ are the two Lewis structures, respectively, for the reactant and the product, while the negative sign is the bonding combination for this case that involves three-electron reorganization.

Subsequently, the Lewis state is further mixed with the remaining two structures $\Phi_i(ex)$, **7** and **8**, to generate the full

(82) (a) Van Lenthe, J. H.; Balint-Kurti, G. G. *Chem. Phys. Lett.* **1980**, *76*, 138−142. (b) Van Lenthe, J. H.; Balint-Kurti, G. G. *J. Chem. Phys.* **1983**, *78*, 5699−5713. (c) Verbeek, J.; Van Lenthe, J. H. *J. Mol. Struct. (THEOCHEM)* **1991**, *229*, 115−137.

(83) Song, L.; Wu, W.; Mo, Y.; Zhang, Q. *XMVB*, an ab Initio Nonorthogonal Valence Bond Program; Xiamen University: Xiamen, China, 1999.

(84) Frisch, M. J.; Trucks, G. W.; Schlegel, H. B.; Scuseria, G. E.; Robb, M. A.; Cheeseman, J. R.; Zakrzewski, V. G.; Montgomery, J. A., Jr.; Stratmann, R. E.; Burant, J. C.; Dapprich, S.; Millam, J. M.; Daniels, A. D.; Kudin, K. N.; Strain, M. C.; Farkas, O.; Tomasi, J.; Barone, V.; Cossi, M.; Cammi, R.; Mennucci, B.; Pomelli, C.; Adamo, C.; Clifford, S.; Ochterski, J.; Petersson, G. A.; Ayala, P. Y.; Cui, Q.; Morokuma, K.; Malick, D. K.; Rabuck, A. D.; Raghavachari, K.; Foresman, J. B.; Cioslowski, J.; Ortiz, J. V.; Stefanov, B. B.; Liu, G.; Liashenko, A.; Piskorz, P.; Komaromi, I.; Gomperts, R.; Martin, R. L.; Fox, D. J.; Keith, T.; Al-Laham, M. A.; Peng, C. Y.; Nanayakkara, A.; Gonzalez, C.; Challacombe, M.; Gill, P. M. W.; Johnson, B. G.; Chen, W.; Wong, M. W.; Andres, J. L.; Head-Gordon, M.; Replogle, E. S.; Pople, J. A. *Gaussian 98*, revision A.10; Gaussian, Inc.: Pittsburgh, PA, 1998.

(85) (a) Shaik, S.; Ioffe, A.; Reddy, A. C.; Pross, A. *J. Am. Chem. Soc.* **1994**, *116*, 262−273. (b) Reddy, A. C.; Shaik, S. *J. Chem. Soc., Faraday Trans.* **1994**, *90*, 1631−1642.

***Table 1.*** Computed Barriers ($\Delta E^{\ddagger}$) for the Nonidentity Reaction, X• + H−H′ → X−H + •H′; X = (F, Cl, Br, I) (in kilocalories per mole)

| | UHF | MP2 | CCSD (T) | VBSCF (TS) | VBSCF (ACS) | BOVB (TS) | BOVB (ACS) | VBCI (TS) | VBCI (ACS) |
|---|---|---|---|---|---|---|---|---|---|
| F | 30.6 | 8.3 | 6.0 | 24.4 | 24.4 | 7.6 | 7.4 | 6.4 | 4.5 |
| Cl | 24.2 | 16.1 | 16.9 | 31.7 | 31.5 | 18.9 | 18.2 | 18.7 | 18.4 |
| Br | 31.4 | 24.5 | 25.9 | 36.9 | 35.8 | 27.2 | 25.1 | 26.6 | 24.4 |
| I | 38.4 | 34.3 | 35.6 | 43.1 | 40.7 | 35.7 | 31.3 | 35.5 | 31.7 |

***Table 2.*** Geometric Features of the TS and ACS for the Nonidentity Reaction, X• + H−H′ → X−H + •H′; X = (F, Cl, Br, I)

| | | geometric parameters | | | | | | % deviation[a] (ACS vs TS) | | % extension[b] (ACS) | |
|---|---|---|---|---|---|---|---|---|---|---|---|
| | X | TS | | | ACS | | | | | | |
| | | $d$(H–H′) | $d'$(X–F) | $d+d'$ | $d$(H–H′) | $d'$(X–H) | $d+d'$ | % $\Delta(d)$ | % $\Delta(d')$ | % $\Delta d/d_0$ | % $\Delta d'/d'_0$ |
| BOVB | F | 0.8553 | 1.2699 | 2.1252 | 0.8876 | 1.2375 | 2.1255 | 3.8 | −2.5 | 20.4 | 32.5 |
| | Cl | 0.9717 | 1.4437 | 2.4154 | 0.9065 | 1.4916 | 2.3972 | −6.7 | 3.3 | 23.0 | 17.0 |
| | Br | 1.1512 | 1.5133 | 2.6646 | 0.9725 | 1.6148 | 2.5872 | −15.5 | 6.7 | 31.9 | 12.8 |
| | I | 1.2928 | 1.6736 | 2.9664 | 1.0606 | 1.7903 | 2.8509 | −18.0 | 7.0 | 43.8 | 12.1 |
| VBCI | F | 0.7728 | 1.3930 | 2.1657 | 0.8657 | 1.2591 | 2.1248 | 12.0 | −9.6 | 17.4 | 34.8 |
| | Cl | 0.9440 | 1.4632 | 2.4073 | 0.8934 | 1.5018 | 2.3953 | −5.4 | 2.6 | 21.1 | 17.8 |
| | Br | 1.1140 | 1.5324 | 2.6463 | 0.9652 | 1.6193 | 2.5845 | −13.4 | 5.7 | 30.9 | 13.1 |
| | I | 1.2586 | 1.6877 | 2.9463 | 1.0532 | 1.7946 | 2.8478 | −16.3 | 6.3 | 42.8 | 12.4 |

[a] % $\Delta(d) = 100[d(\text{ACS}) - d(\text{TS})]/d(\text{TS})$. [b] % $\Delta d/d_0 = 100[d(\text{ACS}) - d_0]/d_0$.

adiabatic state that corresponds to the ACS geometry:

$$\Psi_{\text{ACS}} = c_{\text{L}}\Psi_{\text{L}} + c_7\Phi_7(\text{ex}) + c_8\Phi_8(\text{ex}) \qquad (13)$$

The individual covalent and ionic components of the Lewis state are fully optimized during the calculations, so that the final adiabatic ACS is the variational mixture of all the eight structures in the VB structure set in Scheme 1.

The purely covalent structures, also called Heitler−London (HL) structures, cross along the IRC and thereby generate the backbone of the state crossing in the VBSCD. The combination of the HL structures at the crossing point is called the HL state, given by eq 14:

$$\Psi_{\text{HL}} = c_{\text{r}}\Phi_{\text{HL}}(\text{r}) - c_{\text{p}}\Phi_{\text{HL}}(\text{p}) \qquad (14)$$

Thus, while $\Psi_{\text{HL}}$ accounts for the covalent three-electron delocalization over the three reacting atoms, $\Psi_{\text{L}}$ simply adds the contribution of the ionic fluctuations (**3**−**6**) into the two-electron bonds. The mixing of **7** and **8** further contributes to the ACS by adding the charge-transfer fluctuations from one two-electron bond to the other. The energetic effect imparted by mixing of the ionic structures is given by the resonance energy due to covalent-ionic mixing in eq 15.[70]

$$\text{RE}_{\text{cov-ion}} = E(\Psi_{\text{ACS}}) - E(\Psi_{\text{HL}}) \qquad (15)$$

This quantity is therefore a direct measure of the "polar effect" in the ACS and hence also in the TS, provided the two states are sufficiently close.

**Results.** Table 1 shows the energy barriers of the reactions, of eq 3, with various methods. The well-established accurate CCSD(T) method can be taken as a reference, while unrestricted Hartree−Fock (UHF) and MP2 results are also included to gauge the effects of electron correlation. The barriers of the MO-based methods, UHF, MP2, and CCSD(T) are computed only at the TS geometries, while VBSCF, BOVB, and VBCISD calculations are carried out for both the TS and ACS geometries. It can be seen from Table 1 that the UHF and VBSCF barriers are poor. For F, the UHF barrier is 30.6 kcal/mol, and the VBSCF is 24.4 kcal/mol; both are much higher than the 6.0 kcal/mol obtained with CCSD(T) and 6.4 kcal/mol with VB-CISD. This is because the UHF method does not describe the electronic correlation, while the VBSCF method lacks dynamic correlation, which is essential for the accuracy of the calculations. The barriers of BOVB and VBCISD are in reasonably good agreement with those of the MO-based CCSD(T) method. The VBCISD barriers match CCSD(T) results very well; the deviations between the CCSD(T) and VBCISD barriers are 0.4, 1.8, 0.7, and 0.1 kcal/mol for X = F, Cl, Br, I, respectively. This reconfirms the previous observations that VBCISD is equivalent to the level of CCSD(T) for describing electronic correlation.[78]

The match between the barriers at the TS and ACS is not uniform; at the VBCISD level the deviation spreads from 0.3 kcal/mol for Cl to 3.8 kcal/mol for I, while at the BOVB level, the spread is from 0.2 kcal/mol for F to 4.4 kcal/mol for I. However, *in terms of relative energies*, the trend in the ACSs reflects well the trend in the TSs. All levels of calculations share the same trend for the barriers; it increases with the decrease of electronegativity of X, which implies already that polar effects in this series are variable.

Table 2 shows key geometric features of the TS and the ACS at the VBCI and BOVB levels. Save some small differences, the VBCI and BOVB results exhibit the same trends in the geometry of the ACS. The bond lengths in the TS and ACS are seen to differ by 3.8−18.0% for H−H′ and 2.5−9.6% for X−H. Although these deviations are not negligible, it can be seen that the sum of the distances in the TS and ACS is quasi-constant. This means that the ACS lies on the reaction coordinate and is displaced relative to the TS in a "Hammond fashion",[86] so that the total length of the X- - -H- - -H′ species is conserved. As shown previously, this is a general phenomenon, and one can locate the ACS by starting at the TS and stepping along the reaction vector, which is the eigenmode having an imaginary frequency in the TS.[85] The displacement is therefore linear, and as such the ACS and the TS are both located within the avoided crossing region, *near the flat top of the TS region where the energy variation is moderate*. In fact, the trends in the barriers

(86) Hammond, G. S. *J. Am. Chem. Soc.* **1955**, *77*, 334−338.

of the TS and ACS are the same and so are the geometric trends. Thus, inspecting the H- - -H′ distance variation shows that the bond gets increasingly longer in the series from X = F to X = I, in both the TS and the ACS. This trend that follows the Hammond[86] postulate about the variation of the TS geometry as a function of the reaction driving force further indicates the kinship of the ACS and TS and provides a further incentive for using the ACS as an approximation to the TS.

Table 2 shows also the extension values (in %) of the two bonds in the ACS relative to the equilibrium bond lengths of the ground-state molecules H−H′ and X−H. One can see that the greater the extension values of H−H bond lengths, the higher the barriers.

Table 3 lists structural weights of the VB structures at the ACS. The weights of structures are categorized as covalent ($\omega_{cov}$) and ionic ($\omega_i$); the latter is subdivided into ionic structures that contribute to the bonds of reactants and products (r, p: structures **3**−**6** in Scheme 1) and excited ionic structures (ex: structures **7**, **8**). It can be seen that for all three levels the ACS species are primarily covalent, but all have significant ionic contributions that amount to as much as 30−43% of the total weight. As X is varied from F to I, the ionicity is decreased, while the covalency is increased. This phenomenon is also manifested in the covalent-ionic resonance energy, $RE_{cov-ion}$, which decreases from F toward I. Clearly, in this series the "polar effect" is variable and follows the electronegativity of X.

**A Semiempirical VB Analysis. The Condition for Crossing at the ACS.** The ab initio VB results may be analyzed by use of the following semiempirical VB ideas. The energies of two Lewis structures at the ACS are equal, that is,

$$E(\Phi_L(r), X^{\bullet}\ H{-}H)^{\ddagger} = E(\Phi_L(p), X{-}H\ {}^{\bullet}H)^{\ddagger} \qquad (16)$$

where the double dagger refers to the structures at their ACS geometries. The condition for achieving this energy equality can be derived using expressions of the semiempirical VB method employed before in a similar analysis. As discussed in previous articles,[73] the energies of the two Lewis structures are expressed in eqs 17a and 17b,

$$E(\Phi_L(r), X^{\bullet}\ H{-}H')^{\ddagger} = -\lambda(H{-}H') + 0.5[\lambda_T(X,H) + \lambda_T(X,H')]^{\ddagger} \quad (17a)$$

$$E(\Phi_L(p), X{-}H\ {}^{\bullet}H')^{\ddagger} = -\lambda(H{-}X) + 0.5[\lambda_T(H,H') + \lambda_T(X,H')]^{\ddagger} \quad (17b)$$

where $\lambda$ is the bond energy, while $\lambda_T$ refers to the triplet repulsion. The condition for crossing becomes then eq 18:

$$-\lambda(H{-}H')^{\ddagger} + 0.5\lambda_T(X,H)^{\ddagger} = -\lambda(H{-}X)^{\ddagger} + 0.5\lambda_T(H,H')^{\ddagger} \quad (18)$$

Table 4 shows the semiempirical quantities evaluated using VBCI calculations on the ACS structures of this study. For the VBCI method, it can be seen that in three cases the condition of eq 18 is reasonably met, while for the HHF case there is a discrepancy of 5.2 kcal/mol, which may reflect the neglect of the electrostatic and steric interactions in eqs 17a and 17b.

***Table 3.*** VB Calculated Quantities for the ACS: Weights ($\omega$) of Covalent and Ionic Structures, $RE_{cov-ion}$ Values (in kilocalories per mole)

| X | | F | Cl | Br | I |
|---|---|---|---|---|---|
| VBSCF | $\omega_{cov}$ | 0.6168 | 0.6017 | 0.6391 | 0.6890 |
| | $\omega_i$(r,p) | 0.3250 | 0.3193 | 0.2855 | 0.2413 |
| | $\omega_i$(ex) | 0.0582 | 0.0790 | 0.0754 | 0.0697 |
| BOVB | $\omega_{cov}$ | 0.5706 | 0.5905 | 0.6241 | 0.6593 |
| | $\omega_i$(r,p) | 0.3863 | 0.3776 | 0.3324 | 0.2988 |
| | $\omega_i$(ex) | 0.0431 | 0.0319 | 0.0435 | 0.0420 |
| VBCI | $\omega_{cov}$ | 0.5704 | 0.6528 | 0.6621 | 0.7017 |
| | $\omega_i$(r,p) | 0.3528 | 0.2645 | 0.2653 | 0.2321 |
| | $\omega_i$(ex) | 0.0768 | 0.0823 | 0.0727 | 0.0662 |
| $RE_{cov-ion}$ | VBSCF | 39.7 | 34.3 | 26.7 | 19.5 |
| | BOVB | 48.5 | 38.5 | 30.0 | 23.6 |
| | VBCI | 49.4 | 36.4 | 29.1 | 22.1 |

***Table 4.*** Semiempirical Values Obtained from VBCI Calculation in the ACS (in kilocalories per mole)

| | F | | Cl | | Br | | I | |
|---|---|---|---|---|---|---|---|---|
| | H–F | H–H | H–Cl | H–H | H–Br | H–H | H–I | H–H |
| $\lambda$ | 97.8 | 92.9 | 83.7 | 90.9 | 74.7 | 85.0 | 64.5 | 76.7 |
| $\lambda_T$ | 91.2 | 111.5 | 115.6 | 104.5 | 107.6 | 88.4 | 91.2 | 72.0 |
| $E_r$ | −47.3 | | −33.1 | | −31.2 | | −31.1 | |
| $E_p$ | −42.1 | | −31.5 | | −30.5 | | −28.6 | |
| $\Delta E_{ST}$ | 361.2 | 248.7 | 315.9 | 248.7 | 259.2 | 248.7 | 217.3 | 248.7 |
| $D_e$[a] | 127.3 | 97.4 | 94.9 | 97.4 | 80.7 | 97.4 | 68.3 | 97.4 |
| $D_e$[b] | 140.2 | 109.4 | 107.2 | 109.4 | 93.8 | 109.4 | 81.1 | 109.4 |
| $\Delta E^{\ddagger}$ | 4.5 | | 18.4 | | 24.4 | | 31.7 | |

[a] VBCI calculation. [b] Refernce 15a.

Comparison of the $\lambda$ values of the ACS with the bond dissociation energies, $D_e$, of the ground-state molecules leads to the conclusion that to attain the energy equality in the ACS (eq 18), the stronger of the two bonds has to be weakened much more than the weaker one. At the limit, we might consider that the weak bond will retain its original strength while the strong bond will have to stretch to achieve bond strength equality with the weak bond. The case of X = I almost reaches this virtual limit. Thus, we should expect that *the properties of the TS (ACS) would be mostly controlled by the weak bond.*

**The Resonance Energy of the ACS.** The resonance energy of the ACS is defined as

$$B = E(\Psi_{ACS}) - E(\Phi_{L,cross}) \qquad (19)$$

where the second term in the expression of $B$ is the energy of $\Phi_L(r)$ or $\Phi_L(p)$ at the crossing point of the diabatic curves (see Figure 1), while the first term is the energy of the ACS. If the ACS is approximated only by the Lewis state (eq 12), a related quantity is $B_L$, which is called the resonance energy of Lewis state and is given as

$$B_L = E(\Psi_{L(ACS)}) - E(\Phi_{L,cross}) \qquad (20)$$

The difference $B - B_L$ will account for the importance of the mixing of the excited ionic structures (**7** and **8**).

The resonance energies of the ACS, $B$, are collected in Table 5. For a given halogen X, one can see the following trend: $B$(BOVB) ≈ $B$(VBCI) > $B$(VBSCF). Thus, while the VBCI and BOVB values are very close to each other, the VBSCF level underestimates all the resonance energies.[87] Nevertheless, irrespective of the method, $B$ is seen to decrease generally from F to I, but the $B$ values of Cl and F are oddly almost identical.

***Table 5.*** VB Calculated Resonance Energy *B* in the ACS and Semiempirical *B* Values Obtained from VBCI Calculation (in kilocalories per mole)

| | X | F | Cl | Br | I |
|---|---|---|---|---|---|
| *B* | VBSCF | 40.5 | 42.8 | 37.9 | 31.8 |
| | BOVB | 49.7 | 51.3 | 44.7 | 37.7 |
| | VBCI | 49.0 | 49.0 | 43.6 | 36.5 |
| $B_L$ | VBSCF | 35.4 | 35.6 | 31.7 | 26.7 |
| | BOVB | 40.1 | 41.9 | 38.1 | 32.7 |
| | VBCI | 40.0 | 41.8 | 38.0 | 32.4 |
| $B - B_L$ | VBSCF | 5.1 | 7.2 | 6.2 | 5.1 |
| | BOVB | 9.6 | 9.4 | 6.6 | 5.0 |
| | VBCI | 9.0 | 7.2 | 5.6 | 4.1 |
| *B* | eq 22 | 48.7 | 47.4 | 43.0 | 37.1 |
| | eq 23 | 49.2 | 49.3 | 44.5 | 38.1 |
| | eq 24 | 48.7 | 47.5 | 40.4 | 34.2 |

The $B_L$ quantity in Table 5 exhibits the same trend as *B*, decreasing from F to I and being almost equal for F and Cl. The difference quantity, $B - B_L$, that accounts for the mixing of the excited ionic structures is of the order of 4.1−9.6 kcal/mol, which is more significant and more variable than previously computed for the nonidentity series defined by eq 2, $X' \neq X = CH_3$, $SiH_3$, $GeH_3$, $SnH_3$, $PbH_3$.[73] Thus, once again we see in the present series a clear trend of the "polar effect" that depends on electronegativity.

Using semiempirical VB theory, we can derive an expression for *B*, based on the mixing of the two VB structures. The details are given in Appendix 2 of ref 73, while eq 21 shows the result:

$$B = 1/3[\lambda(\mathrm{H-X}) + 0.5\lambda_T(\mathrm{H,X}) - 0.5\lambda_T(\mathrm{X,H'}) - \lambda(\mathrm{X-H'})]^{\ddagger} \quad (21)$$

Neglecting the long-range terms, the expression for *B* becomes

$$B = 1/3[\lambda(\mathrm{H-H'}) + 0.5\lambda_T(\mathrm{H-H'})]^{\ddagger} = 1/3[\lambda(\mathrm{H-X}) + 0.5\lambda_T(\mathrm{H-X})]^{\ddagger} \quad (22)$$

Since the difference of $[\lambda + \lambda_T]^{\ddagger}$ between pairs (H,H′) and (H,X) is small (see Table 4), we used an average $\lambda$ value for *B*. The so estimated (eq 22) *B* values are presented in Table 5, along with the VB calculated quantities. The match between the calculated values to the estimated ones is seen to be reasonably good.

Since the $\lambda$ and $\lambda_T$ parameters of the bonds (H−H or H−X) can be approximated as half the singlet−triplet energy $\Delta E_{ST}$, the expression for the resonance energy can be simplified as in eq 23:

$$B = 0.25\Delta E_{ST}(\mathrm{H-H'})^{\ddagger} = 0.25\Delta E_{ST}(\mathrm{H-X})^{\ddagger} \quad (23)$$

where the double dagger corresponds to the ACS geometry. Considering the rough equality of the excitation energies for the two bonds, in the ACS (see $\lambda_T$ VBCI values in Table 4) eq 23 can be used with an average of the two quantities. Alternatively, using the fact that the weakest bond is not much elongated in the ACS (see above), one can determine *B* as one-half of the bond energy of the weaker of the two bonds, as in eq 24:

$$B \approx 0.5D(\mathrm{H-H'}), \quad \text{for X = F;}$$
$$B \approx 0.5D(\mathrm{H-X}), \quad \text{for X = Cl, Br, and I} \quad (24)$$

The advantage of eq 24 (which is obviously restricted to nonidentity reactions) over eqs 22 and 23 is that it deals with an easily accessible quantity, the bond energy of a molecule in its equilibrium geometry, while eqs 22 and 23 deal with quantities that have to be evaluated at the ACS geometry. The *B* values calculated directly from the VB calculations (see Figure 1) and from the semiempirical relations in eqs 22−24 are collected in the last three lines in Table 5. It can be seen that the semiempirical equations for *B* are quite consistent and lead to values close to those calculated with BOVB and VBCI.

To further demonstrate the generality of the semiempirical derivations, we gather in Table 9 the entire set of computed and semiempirically estimated *B* values for nonidentity reactions (2) ($X' \neq X = CH_3$, $SiH_3$, $GeH_3$, $SnH_3$, and $PbH_3$) and (3) (X = F, Cl, Br and I), the former set arising from a previous study.[73] Since the previous study was carried out with BOVB, the entire set is given here only for this method. It is apparent that the semiempirical eqs 22 and 24 work rather well for a highly variable set of X, X′ groups.

**Reaction Barriers.** Modeling of reaction barrier is a primary goal for a theoretical study. In this article, we use ACS to characterize the TS and model the barrier. From Figure 1, the barrier is given as:

$$\Delta E^{\ddagger} = \Delta E_c - B \quad (25)$$

where $\Delta E_c$ is the height of the crossing point and *B* is the resonance energy discussed above.

The height of the crossing point is given by the energy difference of the Lewis structure at the ACS geometry vs the ground-state geometry (see Figure 1). As done for the resonance energy, let us first use the semiempirical VB method to rationalize the height of the crossing point $\Delta E_c$. Using the Lewis structure with the H−H′ bond, the height of the crossing point is given as:[73]

$$\Delta E_c = \lambda(\mathrm{H-H})_0 - \lambda(\mathrm{H-H'})^{\ddagger} + 0.5[\lambda_T(\mathrm{X,H}) + \lambda_T(\mathrm{X,H'})]^{\ddagger} \quad (26)$$

The values of $\Delta E_c$ obtained from eq 26 are listed in Table 6. It is shown that the semiempirical VB results match the ab initio VBCI results; the errors are in the range of 1.2−3.5%.

An alternative way to evaluate the height of the avoided crossing is from the VB parameters in VBSCD. For an identity reaction, the height of the crossing point is related to the promotion gap of the VBSCD as follows:[67]

$$\Delta E_c = fG \quad (27)$$

where *f* is the fraction factor of the promotion gap, *G*, that separates the two Lewis curves at their onset ($Q = \pm 1$) in Figure 1. For a nonidentity reaction, shown in Figure 1, the promotion gap *G* and curvature factors *f* are different for the reactants and products. Another factor is the reaction driving force, given by

(87) This is a general tendency that can be easily understood in the simple case of a resonance between two VB structures. For the diabatic curves, each represented by a single VB stsructure, the VBSCF and BOVB levels are equivalent. By contrast, these two levels become nonequivalent in the ground state, which is described by two structures. In this latter state, the breathing-orbital effect is at work and the BOVB energy is lower than the VBSCF energy, thus yielding larger resonance energy as a systematic tendency.

***Table 6.*** Comparison of Heights of the Crossing Points (in kilocalories per mole) for the Nonidentity Reaction, X• + H−H′ → X−H + •H′; X = (F, Cl, Br, I), Computed by VBCI and Some Semiempirical Model Equations

| | HHF | HHCl | HHBr | HHI |
|---|---|---|---|---|
| $\Delta E_c$(VBCI) | 53.4 | 67.4 | 67.9 | 68.4 |
| $\Delta E_c$(eq 26) | 52.7 | 65.1 | 66.6 | 67.6 |
| % error (vs VBCI) | −1.5 | −3.5 | −2.0 | −1.2 |
| $\Delta E_c$(eq 29) | 57.2 | 68.9 | 69.4 | 73.1 |
| % error (vs VBCI) | 6.9 | 2.2 | 2.2 | 6.7 |
| $\Delta E_c$(eq 31) | 59.7 | 68.7 | 68.2 | 71.3 |
| % error (vs VBCI) | 11.6 | 1.9 | 0.4 | 4.1 |

***Table 7.*** Reactivity Factors and Heights of the Crossing Points (in kilocalories per mole) Calculated from the VBSCD and by Direct VBCI Computations

| X | $f$ | $f'$ | $G$ | $G'$ | $\Delta E_c$ | $\Delta E_{rp}$ | $f_a$ | $G_a$ | $\Delta E^{\ddagger}$ (eq 32) |
|---|---|---|---|---|---|---|---|---|---|
| F | 0.37 | 0.28 | 163.0 | 303.3 | 53.5 | −29.9 | 0.32 | 233.4 | 10.7 |
| Cl | 0.36 | 0.32 | 167.2 | 229.7 | 67.4 | 2.5 | 0.34 | 198.3 | 19.7 |
| Br | 0.38 | 0.30 | 167.2 | 185.0 | 67.9 | 16.7 | 0.34 | 176.1 | 24.6 |
| I | 0.42 | 0.29 | 167.2 | 147.9 | 68.4 | 29.1 | 0.36 | 157.5 | 34.8 |

the difference in the corresponding bond energies of reactants and products:

$$\Delta E_{rp} = E(\mathrm{r}) - E(\mathrm{p}) = D(\mathrm{H{-}H'}) - D(\mathrm{X{-}H}) \quad (28)$$

Taking all these factors into a single equation, an expression for the height of crossing point, $\Delta E_c$, was derived before as:[73]

$$\Delta E_c = f_a G_a + (G'/2G_a)\Delta E_{rp} + (1/2G_a)\Delta E_{rp}^{\ 2} \quad (29)$$

where the average gap $G_a$ and $f_a$ are defined as:

$$G_a = 0.5(G + G'), \quad f_a = 0.5(f + f') \quad (30)$$

A more compact expression can be given by neglecting the quadratic term in eq 29 and taking $G'/2G_a$ as ∼1/2:

$$\Delta E_c = f_a G_a + 0.5\Delta E_{rp} \quad (31)$$

The heights of the crossing points $\Delta E_c$ for the set of reactions (3), as calculated by use of eqs 26, 29, and 31, are listed in Table 6, with the deviations compared to the corresponding ab initio VBCI computed values. It can be seen that eq 26 reproduces the ab initio computed values quite well. Remarkably, *eq 29 that only uses fundamental parameters of the VBSCD, which arise from properties of the reactants and products in their equilibrium geometries, performs fairly well*. Equation 31, which is a simplified version of eq 29, is a little less accurate, as expected, but correctly reproduces the tendencies from X = F to X = I. The same data for reaction 2, arising from our previous studies, are listed in Table 10 later. A linear regression analysis with all the data for the two reaction series reveals that the semiempirically estimated heights of the crossing point correlate well with the VB computed ones, e.g., $R^2$ values are 0.9848 for eq 26, 0.9664 for eq 29, and 0.9610 for eq 31. All in all, eq 31 appears to be a good approximation for eq 29 and reproduces ab initio results fairly well.

The quantities $G$, $G'$, and $\Delta E_{rp}$ are available directly from the VB calculations and are shown in Table 7. The $f$ and $f'$ are derived from the VB curves at $Q = 0$.[73] It can be seen that the $G$ values are virtually constant as they should be, since, in all the reactions, these are related to the singlet−triplet excitation energy of the H−H bond; the slight difference between F and the others are due to basis sets. On the other hand, the quantity $G'$ decreases down a column of the periodic table, since it reflects the promotion energy of H−X bond, which decreases from F to I. The average quantity $f_a$ is less variable, and its values, $f_a = 0.32-0.36$, are approximately the same as those previously studied[73] and close also to the values in the identity reactions.[70] This quasi-constancy of the factor $f_a$ for a given family of reactions, here the hydrogen abstraction reactions, which has long been a working hypothesis in qualitative applications of the VBSCD[67,68] model, is nicely confirmed here and may lead, as will be seen later, to further simplified semiempirical equations for estimating barrier heights.

***Table 8.*** Comparison of ab Initio VBCI Calculated Barriers with Semiempirical Equations (in kilocalories per mole)

| entry | X,X′ | H,F | H,Cl | H,Br | H,I |
|---|---|---|---|---|---|
| 1 | $\Delta E^{\ddagger}$(VB,ACS) | 4.5 | 18.4 | 24.4 | 31.7 |
| 2 | $\Delta E^{\ddagger}$ (VB,TS) | 6.4 | 18.7 | 26.6 | 35.5 |
| 3 | $\Delta E^{\ddagger}$ (eq 32) | 10.7 | 19.7 | 24.6 | 34.8 |
| 4 | $\Delta E^{\ddagger}$ (Marcus) | 9.5 | 25.5 | 28.6 | 34.8 |
| 5 | $\Delta E^{\ddagger}$ (eq 39) | 11.3 | 17.9 | 27.4 | 35.6 |
| 6 | $\Delta E^{\ddagger}_{int}$ (eq 38) | 26.2 | 16.7 | 19.0 | 21.1 |
| 7 | $\Delta E^{\ddagger}_{int}$ (eq 34) | 25.7 | 18.4 | 16.3 | 20.2 |

Using eq 31, we can derive a compact expression for the energy barrier:[73]

$$\Delta E^{\ddagger}(\mathrm{VBSCD}) = f_a G_a + 0.5\Delta E_{rp} - B \quad (32)$$

Equation 32 shows that the barrier is a balance between an intrinsic term, $f_a G_a$, and the reaction "driving force" term, $\Delta E_{rp}$. The validity of eq 32 can be appreciated by comparing entries 2 and 3 in Table 8, which displays some calculated barriers for the set of reactions (3) with X = F, Cl, Br, and I, while corresponding data for X = $CH_3$, $SiH_3$, $GeH_3$, $SnH_3$, and $PbH_3$ from the previous study are displayed in Table 11 later. With one exception for X = F (where eq 32 overestimates the barrier by 4.3 kcal/mol), it can be seen that eq 32 reproduces the VB calculated barriers with reasonable accuracy. This agreement is graphically illustrated in Figure 2a, which shows a plot of the VBSCD-derived barriers (eq 32) against the VB calculated barriers for the entire set of identity and nonidentity reactions in eqs 1−3.

It is interesting to compare eq 32 with the Marcus expression[76] for the barrier, in terms of the intrinsic barrier, $\Delta E_0^{\ddagger}$, and the reaction energy, $\Delta E_{rp}$, as shown in eq 33.

$$\Delta E^{\ddagger}(\mathrm{Marcus}) = \Delta E_0^{\ddagger} + 0.5\Delta E_{rp} + \Delta E_{rp}^{\ 2}/16\Delta E_0^{\ddagger} \quad (33)$$

In the Marcus equation, the intrinsic barrier $\Delta E_0^{\ddagger}$, which is the "pure kinetic" barrier without the effect of the thermodynamics of the process, is determined as the average of the component identity barriers. However, the intrinsic barrier in the VBSCD may be defined in explicit terms, by

$$\Delta E_{int}^{\ddagger} = f_a G_a - B \quad (34)$$

Thus, the VBSCD barrier becomes eq 35:

$$\Delta E^{\ddagger}(\mathrm{VBSCD}) = \Delta E_{int}^{\ddagger} + 0.5\Delta E_{rp} \quad (35)$$

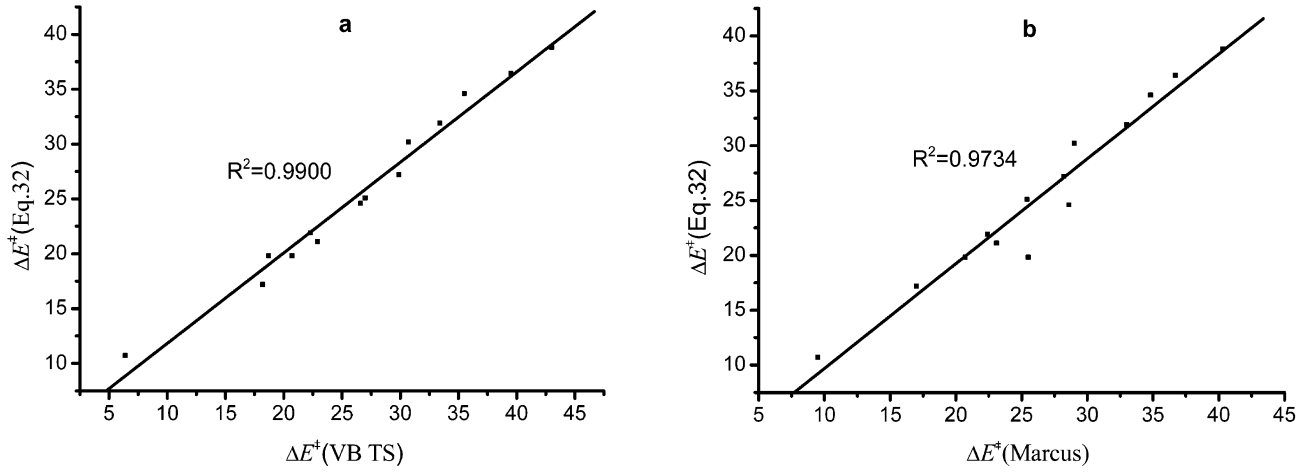


***Figure 2.*** VBSCD-derived barriers (eq 32) plotted (a) against the VB calculated barriers and (b) against the Marcus equation for the entire set of identity and nonidentity reactions. Energies in kcal/mol.

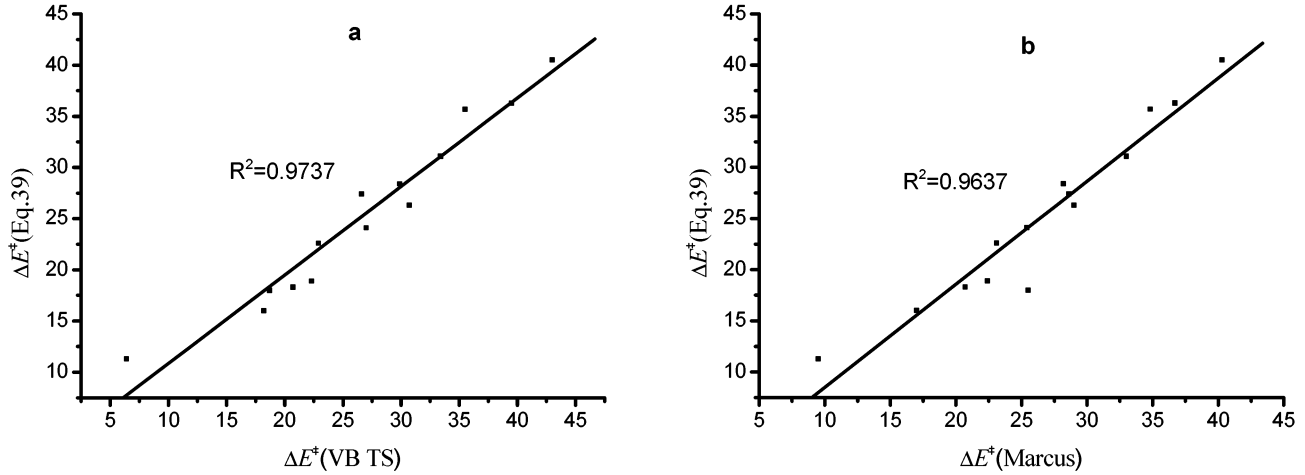


***Figure 3.*** VBSCD-derived barriers (eq 39) plotted (a) against the VB calculated barriers and (b) against Marcus equation for the entire set of identity and nonidentity reactions. Energies in kcal/mol.

where it is described as the "pure kinetic" barrier, the intrinsic barrier, attenuated by the reaction thermodynamic quantity.

Tables 8 and 11 as well as Figure 2b show the correlation between eq 32 and the Marcus equation (eq 33). Clearly, eq 32 and the corresponding equation for the identity reaction (eq 34), which are based on the VBSCD, capture the key factors determining the barrier.

An added feature of the VBSCD equation is the ability to calculate directly the intrinsic barrier quantity, using eq 34. Owing to the quasi-constancy of the $f_a$ factor in hydrogen abstraction reactions (see above), the intrinsic barrier is seen to be determined only by the promotion gaps, $G$ and $G'$, in Figure 1 (Table 7), and the resonance energy $B$. As noted already, the gaps can be related to the corresponding bond energies by the following relationship:

$$G_a = 0.5\,(G + G') \approx D(\mathrm{H{-}H'}) + D(\mathrm{H{-}X}) \qquad (36)$$

Similarly, the resonance energy $B$ is related to the bond energies of the weak bond as shown above in eq 24. Using these relations, the intrinsic barrier is seen to depend on the combination of bond energies as follows:

$$\Delta E^{\ddagger}_{\mathrm{int}} = f_a(D(\mathrm{H{-}H'}) + D(\mathrm{H{-}X})) - 0.5D_W \qquad (37)$$

where $D_W$ means the weaker bond energy. Taking the qualitatively derived $f_a$ value of 1/3, eq 37 is written as follows:

$$\Delta E^{\ddagger}_{\mathrm{int}} = K(D_S - 0.5D_W); \quad K = 1/3 \qquad (38)$$

where $D_S$ is the stronger bond energy. Using eqs 35 and 38, an approximate expression for barrier is given as:

$$\Delta E = K(D_S - 0.5D_W) + 0.5\Delta E_{rp}; \quad K = 1/3 \qquad (39)$$

As the reaction driving force, $\Delta E_{rp}$, is itself simply expressed as $\pm(D_S - D_W)$ depending on whether the reaction is endo- or exothermic, eq 39 expresses the barrier as a function of a two easily accessible quantities: the bonding energies of the reactants and products. The intrinsic barriers computed by eq 38 and the VBSCD barrier computed by eq 39 are listed in Table 8. It can be seen that they are in good agreements with the computed VBCI values. Figure 3 shows the correlation between the barriers of eq 39 and the computed VBCI barriers of the TS (Figure 3a) and Marcus equation (Figure 3b). The plot shows that eq 39 provides the direct insight into the relationship between bond energy and reaction barrier.

Clearly, the general correlation further strengthens the importance of the reaction energy as one of the determinants

***Table 9.*** Comparison of ab Initio BOVB Calculated *B* Values with Semiempirical Equations for Reaction 3 with X = F, Cl, Br, I, and Reaction 2[a] with X ≠ X′ = $CH_3$, $SiH_3$, $GeH_3$, $SnH_3$, $PbH_3$ (in kilocalories per mole)

| | $X^{\bullet} + H–H' \rightarrow X–H + H'^{\bullet}$ | | | | $X'^{\bullet} + H–X \rightarrow X'–H + X^{\bullet}$ | | | | | | | | | |
|---|---|---|---|---|---|---|---|---|---|---|---|---|---|---|
| X,X′ | F | Cl | Br | I | C,Si | C,Ge | C,Sn | C,Pb | Si,Ge | Si,Sn | Si,Pb | Ge,Sn | Ge,Pb | Sn,Pb |
| *B* | 49.7 | 51.3 | 44.7 | 37.7 | 40.0 | 38.9 | 33.7 | 31.4 | 38.8 | 34.2 | 31.5 | 35.0 | 32.4 | 31.9 |
| $B_L$ | 40.1 | 41.9 | 38.1 | 32.7 | 34.7 | 33.4 | 29.0 | 27.1 | 34.2 | 30.2 | 27.6 | 30.4 | 28.0 | 27.8 |
| *B* (eq 22) | 44.5 | 43.7 | 39.6 | 34.5 | 39.0 | 36.4 | 32.4 | 29.7 | 35.8 | 32.0 | 29.2 | 31.8 | 29.3 | 29.2 |
| *B* (eq 24) | 47.0 | 43.5 | 37.1 | 31.5 | 42.1 | 38.8 | 34.2 | 30.8 | 38.8 | 34.2 | 30.8 | 34.2 | 30.8 | 30.8 |

[a] Reference 73.

***Table 10.*** Comparison of ab Initio BOVB Calculated $\Delta E_c$ Values with Semiempirical Equations for Reaction 2[a] with X ≠ X′ = $CH_3$, $SiH_3$, $GeH_3$, $PbH_3$ (in kilocalories per mole)

| X,X′ | C,Si | C,Ge | C,Sn | C,Pb | Si,Ge | Si,Sn | Si,Pb | Ge,Sn | Ge,Pb | Sn,Pb |
|---|---|---|---|---|---|---|---|---|---|---|
| $\Delta E_c$ (VB) | 70.5 | 71.6 | 72.0 | 72.6 | 60.7 | 60.2 | 59.6 | 55.5 | 54.3 | 49.8 |
| $\Delta E_c$ (eq 26) | 74.4 | 72.0 | 74.5 | 73.3 | 57.1 | 59.7 | 58.8 | 54.3 | 52.8 | 46.1 |
| $\Delta E_c$ (eq 29) | 70.1 | 70.9 | 69.8 | 70.2 | 61.1 | 59.5 | 58.8 | 55.1 | 53.5 | 48.9 |
| $\Delta E_c$ (eq 31) | 70.5 | 71.1 | 70.3 | 70.5 | 60.9 | 59.2 | 58.2 | 55.2 | 53.5 | 48.8 |

[a] Reference 73.

***Table 11.*** Comparison of ab Initio BOVB Calculated Barriers with Semiempirical Equations for Reaction 2[a] with X ≠ X′ = $CH_3$, $SiH_3$, $GeH_3$, $SnH_3$, $PbH_3$ (in kilocalories per mole)

| X,X′ | C,Si | C,Ge | C,Sn | C,Pb | Si,Ge | Si,Sn | Si,Pb | Ge,Sn | Ge,Pb | Sn,Pb |
|---|---|---|---|---|---|---|---|---|---|---|
| $\Delta E^{\ddagger}$ (VB ACS) | 30.5 | 32.7 | 38.3 | 41.2 | 21.9 | 26.0 | 28.1 | 20.5 | 22.0 | 17.9 |
| $\Delta E^{\ddagger}$ (VB TS) | 30.7 | 33.4 | 39.5 | 43.0 | 22.3 | 27.0 | 29.9 | 20.7 | 22.9 | 18.2 |
| $\Delta E^{\ddagger}$ (eq 32) | 30.2 | 31.9 | 36.4 | 38.8 | 21.9 | 25.1 | 27.2 | 19.8 | 21.1 | 17.2 |
| $\Delta E^{\ddagger}$ (Marcus) | 29.0 | 33.0 | 36.7 | 40.3 | 22.4 | 25.4 | 28.2 | 20.7 | 23.1 | 17.0 |
| $\Delta E^{\ddagger}$ (eq 39) | 26.3 | 31.1 | 36.3 | 40.5 | 18.9 | 24.1 | 28.4 | 18.3 | 22.6 | 16.0 |
| $\Delta E^{\ddagger}_{int}$ (eq 38) | 19.0 | 20.1 | 21.5 | 22.5 | 15.3 | 16.6 | 17.7 | 14.4 | 15.5 | 12.8 |
| $\Delta E^{\ddagger}_{int}$ (eq 34) | 23.5 | 21.4 | 22.9 | 22.0 | 18.2 | 18.2 | 16.8 | 16.6 | 14.7 | 14.6 |

[a] Reference 73.

of the barrier. However, considering our other correlation of the intrinsic barrier with bond energies, eq 38, *it is apparent that the fundamental factor of the barrier is the promotion energy gap, in the VBSCD, that itself happens to correlate with the bond energy*. Thus, the promotion energy gap provides the cause and causality behind the observed correlation of barriers and bond energies.[50]

One last remark is in order concerning the value of the *K* factor in eqs 38 and 39. This value is based on the calculated $f_a$ factor as calculated for a number of H-abstraction reactions at the VBCI or BOVB levels, in rather modest basis sets. Such calculations are expected to exhibit only fair accuracy, and in particular they would generally tend to *overestimate reaction barriers* and underestimate bond strengths. This means that, while the value 1/3 for the factor *K* is appropriate for correlating barriers to bond strengths as calculated at a modest level, a somewhat smaller value of *K* is probably more appropriate for correlating experimental quantities. In some experimental systems deviations may occur because of changes of the structure of the TS from a linear X- - -H- - -X′ to a bent structure, which should change the values of *B*. Be it as it may, what we wish to stress by use of eq 39 is the existence of a proportionality factor, whatever its value, in a simple expression of the reaction barrier as a function of bond strengths. The results of Mayer[50] indicate that this eq 39 is globally correct.

## Conclusions

The nonidentity hydrogen transfer reactions between H and strongly electronegative groups have been modeled in this work by the reactions $X^{\bullet} + H–H' \rightarrow X–H + H'^{\bullet}$, (X = F, Cl, Br, I), which exhibit a wide spectrum of barriers and endo- or exothermicities. These reactions have been studied by means of various ab initio VB methods, which advantageously provide some insight to the origin of barriers. In this line, the VBSCD model and a semiempirical VB theory have been applied to relate the barriers to easily accessible properties of the reactants and products, on the basis of the VB computational results.

It is not surprising that the VBSCF method cannot provide quantitative accuracy for these kinds of reactions of strongly electronegative atoms because of the lack of dynamic correlation. The BOVB and VBCI methods can give good results, comparable to CCSD(T) using the same basis sets. This shows that the VB method with consideration of dynamic correlation match MO calculations of post-HF methods in accuracy. The VB calculations also permit a clear characterization of the "polar effect", which is due to the mixing of ionic structures in the transition state. Clearly, in the above series the "polar effect" is variable and follows the electronegativity of X.

The combination of the VBSCD model[67] and semiempirical VB theory leads to analytical expressions for the barriers, which match the ab initio VBCI calculations fairly well. This agreement is observed not only for the model reactions that are studied in this work, but also for other identity and nonidentity hydrogen abstraction reactions $X'^{\bullet} + H–X \rightarrow X'–H + X^{\bullet}$, X = (≠) X′ = $CH_3$, $SiH_3$, $GeH_3$, and $PbH_3$ that have been studied in previous articles.[70,71,73] The barriers are seen to be governed by two factors: the endo- or exothermicity of the reaction, $\Delta E_{rp}$, which is the driving force of the reaction, and a fundamental parameter of the VBSCD model, $G_a$, the average singlet−triplet gap of the bonds that are broken or formed in the reactions. Furthermore, as these two parameters are both related to the

bond strengths of the reactants and products, some simplifying assumptions lead to a simple formula (eq 39) *that expresses the barrier for nonidentity hydrogen abstraction as a simple function of the bond strengths of reactants and products.*

The general VBSCD expression for the barrier bears some resemblance with the Marcus equation in terms of $\Delta E_{rp}$ and an intrinsic barrier, but the VBSCD model has the advantage of relating the intrinsic barrier to simple properties of reactants and products. The present work, as well as the results of previous studies, shows that the VBSCD model[67] captures the key factors that determine the barriers of hydrogen abstractions and may relate these barriers to easily accessible properties of the reactants and products, by means of simple analytical expressions.

**Acknowledgment.** The research at XMU was supported by the Natural Science Foundation of China (Nos. 20225311, 20373052, 20021002) and the TRAPOYT of the Ministry of Education of China. The research at HU was supported in part by an Israel Science Foundation (ISF) grant to S.S.

## Appendix

Table 9 shows a comparison of ab initio BOVB calculated *B* values with semiempirical equations for reactions 2 and 3. Table 10 shows a comparison of ab initio $\Delta E_c$ values with semiempirical equations for reaction 2. Table 11 shows a comparison of ab initio BOVB calculated barriers with semiempirical equations for reaction 2.

JA048105F